description of this and the other chromatograms is given in Table 2. Exposure to AAPH results in a pronounced reduction in the amount of HMA, the relative area of its peak decreases from 65.1% to 22.3%. Thus, AAPH is also capable of oxidizing SH-groups of cysteine residues. As mentioned above, in addition to oxidizing the sulfhydryl group of 34-Cys, the reagent also affects other parts of albumin, and this is why we do not observe an increment of one or both of the other peaks in the chromatogram. Instead, the modified HMA elutes as a low, broad peak between 15 and 30 min of elution (not shown). In contrast to HMA, HNA-1 and HNA-2 do not seem to be influenced by AAPH. Fig. 7B proposes that incubating Oct together with AAPH has no influence on HSA-oxidation. This proposal is supported by calculating peak areas (Table 2). By contrast, the presence of *N*-AcTrp has a protecting effect, which is the same whether Oct is present (Fig. 7D) or not (Fig. 7C). The quantitative analysis presented in Table 2 shows that the effect is significant.

Thus, with respect to potential oxidation of HSA, *N*-AcTrp, but not Oct, has a significant protecting effect.

4. Concluding remarks

The annual production of purified HSA now exceeds 300 ton [6]. Therefore, it is surprising that only sparse information can be found about the mechanism of protection of additives during pasteurization and about the potential adverse effects caused by their presence in pharmaceutical-grade HSA. In the present work, we have studied in some detail the effect of additives on the structural and antioxidant properties of HSA. Experiments performed with CD and native-PAGE showed that Oct, and fatty acid anions of a longer chain-length (Fig. 5), has a pronounced stabilizing effect on the structure of monomeric HSA during heating, which also is revealed by higher T_m and ΔH_{cal}-values. *N*-AcTrp binds to the same high-affinity site and has a small additive effect when administered together with Oct. In itself, it has only a minor stabilizing effect. However, no protection during heating was found for L-Trp or *N*-AcCys (Table 1). Thus, the presence of a medium- or long-chain fatty acid is essential for preserving the structure of HSA and for preventing its aggregation during pasteurization.

Apparently, the roles of Oct and *N*-AcTrp for other functional properties of HSA have not been studied before. Interestingly, we found that *N*-AcTrp protects HSA much better than Oct against general oxidation caused by prolonged exposure to AAPH. In contrast to *N*-AcCys, L-Trp also had this effect (Fig. 6). The protection brought about by *N*-AcTrp was pronounced and more immediate in the case of the sulfhydryl group of HSA (Fig. 7). This protective role of *N*-AcTrp can be of practical importance, because 34-Cys of HSA represents the largest fraction of free thiols in blood [4].

Acknowledgements

This work was supported in part by Grants-in-Aid for Scientific Research from the Ministry of Education, Science, Sports and Culture of Japan (11694298; 11794016) and by Aarhus University Research Foundation.

References

[1] S. Curry, H. Mandelkow, P. Brick, N. Franks, Crystal structure of human serum albumin complexed with fatty acid reveals an asymmetric distribution of binding sites, Nat. Struct. Biol. 5 (1998) 827–835.
[2] S. Sugio, A. Kashima, S. Mochizuki, M. Noda, K. Kobayashi, Crystal structure of human serum albumin at 2.5 Å resolution, Protein Eng. 12 (1999) 439–446.
[3] M.L. Ferrer, R. Duchowicz, B. Carrasco, J.G. de la Torre, A.U. Acuna, The conformation of serum albumin in solution: a combined phosphorescence depolarization-hydrodynamic modeling study, Biophys. J. 80 (2001) 2422–2430.
[4] U. Kragh-Hansen, V.T.G. Chuang, M. Otagiri, Practical aspects of the ligand-binding and enzymatic properties of human serum albumin, Biol. Pharm. Bull. 25 (2002) 695–704.
[5] U. Kragh-Hansen, Molecular aspects of ligand binding to serum albumin, Pharmacol. Rev. 33 (1981) 17–53.
[6] T. Peters Jr., All about Albumin: Biochemistry, Genetics, and Medical Applications, Academic Press, San Diego, California, 1996.
[7] E. Bourdon, N. Loreau, D. Blache, Glucose and free radicals impair the antioxidant properties of serum albumin, FASEB J. 13 (1999) 233–244.
[8] R.F. Chen, Removal of fatty acids from serum albumin by charcoal treatment, J. Biol. Chem. 242 (1967) 173–181.
[9] G.A. Picó, Thermodynamic features of the thermal unfolding of human serum albumin, Int. J. Biol. Macromol. 20 (1997) 63–73.
[10] H. Schagger, G. von Jagow, Tricine-sodium dodecyl sulfate-polyacrylamide gel electrophoresis for the separation of proteins in the range from 1 to 100 kDa, Anal. Biochem. 166 (1987) 368–379.
[11] M.M. Bradford, A rapid and sensitive method for the quantitation of microgram quantities of protein utilizing the principle of protein-dye binding, Anal. Biochem. 72 (1976) 248–254.
[12] T. Zor, Z. Selinger, Linearization of the Bradford protein assay increases its sensitivity: theoretical and experimental studies, Anal. Biochem. 236 (1996) 302–308.
[13] E. Niki, Antioxidants in relation to lipid peroxidation, Chem. Phys. Lipids 44 (1987) 227–253.
[14] I. Climent, L. Tsai, R.L. Levine, Derivatization of γ-glutamyl semialdehyde residues in oxidized proteins by fluoresceinamine, Anal. Biochem. 182 (1989) 226–232.
[15] A. Sugii, K. Harada, K. Nishimura, R. Hanaoka, S. Masuda, High performance liquid chromatography of proteins on *N*-methylpyridinium polymer columns, J. Chromatogr. 472 (1989) 357–364.
[16] R. Narazaki, K. Harada, A. Sugii, M. Otagiri, Kinetic analysis of the covalent binding of captopril to human serum albumin, J. Pharm. Sci. 86 (1997) 215–219.
[17] U. Kragh-Hansen, Octanoate binding to the indole- and benzodiazepine-binding region of human serum albumin, Biochem. J. 273 (1991) 641–644.
[18] R.H. McMenamy, J.L. Oncley, The specific binding of L-tryptophan to serum albumin, J. Biol. Chem. 233 (1958) 1436–1447.
[19] T. Kosa, T. Maruyama, M. Otagiri, Species differences of serum albumins: II. Chemical and thermal stability, Pharm. Res. 15 (1998) 449–454.

[20] A. Shrake, J.S. Finlayson, P.D. Ross, Thermal stability of human albumin measured by differential scanning calorimetry. I. Effects of caprylate and *N*-acetyltryptophanate, Vox Sang. 47 (1984) 7–18.
[21] T. Arakawa, Y. Kita, Stabilizing effects of caprylate and acetyltryptophanate on heat-induced aggregation of bovine serum albumin, Biochim. Biophys. Acta 1479 (2000) 32–36.
[22] Y.S. Ma, C.C. Chao, E.R. Stadtman, Oxidative modification of glutamine synthetase by 2,2′-azobis(2-amidinopropane) dihydrochloride, Arch. Biochem. Biophys. 363 (1999) 129–134.
[23] M. Anraku, K. Yamasaki, T. Maruyama, U. Kragh-Hansen, M. Otagiri, Effect of oxidative stress on the structure and function of human serum albumin, Pharm. Res. 18 (2001) 632–639.

Characterization of Site I of Human Serum Albumin Using Spectroscopic Analyses: Locational Relations between Regions Ib and Ic of Site I

KEISHI YAMASAKI,[1] TORU MARUYAMA,[1] AKIRA TAKADATE,[2] AYAKA SUENAGA,[1] ULRICH KRAGH-HANSEN,[3] MASAKI OTAGIRI[1]

[1]Department of Biopharmaceutics, Graduate School of Pharmaceutical Sciences, Kumamoto University, 5-1 Oe-honmachi, Kumamoto 862-0973, Japan

[2]Daiichi College of Pharmaceutical Sciences, 22-1 Tamagawa-cho, Minami-ku, Fukuoka 815-0037, Japan

[3]Department of Medical Biochemistry, University of Aarhus, DK-8000 Aarhus C, Denmark

Received 12 May 2004; revised 21 July 2004; accepted 27 July 2004

Published online in Wiley InterScience (www.interscience.wiley.com). DOI 10.1002/jps.20203

ABSTRACT: Site I of human serum albumin is an important and complex region for high-affinity binding of drugs. Equilibrium dialysis showed independent binding of dansyl-L-asparagine (DNSA) and *n*-alkyl *p*-aminobenzoates (*p*-ABEs) to regions Ib and Ic, respectively, in the pH range 6.0–9.0. However, individual binding of DNSA increased with pH in the same range. Binding of the four *n*-alkyl *p*-ABEs strongly perturbed the circular dichroism spectrum of bound DNSA, and the effect increased with concentration and the number of carbon atoms in the alkyl moiety. A similar effect was observed by increasing pH from 6.0 to 9.0, a pH range in which human serum albumin is known to undergo the neutral-to-base transition. The spectral changes propose spatial orientation changes of DNSA at region Ib. This proposal was supported by increased fluorescence anisotropy values: *n*-alkyl *p*-ABEs binding and the pH-dependent conformational change each restricted the mobility of the naphthalene ring of bound DNSA. Despite the similar effects on the spatial orientation of DNSA, clear differences were observed between the effects of *n*-alkyl *p*-ABEs and neutral-to-base transition. The former hardly changed the affinity and maximum fluorescence emission wavelength of bound DNSA; in contrast, the latter significantly affected them. The results give new information about site I and, according to our knowledge, represent a new type of ligand interaction, because the binding site of DNSA could be changed by simultaneous binding of the *n*-alkyl *p*-ABEs without affecting the binding constant. J Pharm Sci 93:3004–3012, 2004

Keywords: protein binding; albumin; transition; circular dichroism; fluorescence spectroscopy; drug interaction

INTRODUCTION

Modification of drug binding to human serum albumin (HSA) can often change the pharmacokinetics and pharmacological effects of a drug.[1,2] Free drug concentration can be affected by the presence of other drugs or endogenous ligands, or by microenvironmental changes in disease states. Diminished drug binding is usually the result of either competitive displacement from the same binding site or allosteric displacement following microenvironmental changes at the binding site. Many drugs bind with high affinity to one of the sites of HSA.[1,3] In their classical work, Sudlow et al.[4,5] characterized two sites for drug binding,

Correspondence to: Masaki Otagiri (Telephone: 81-96-371-4150; Fax: 81-96-362-7690;
E-mail: otagirim@gpo.kumamoto-u.ac.jp)

Journal of Pharmaceutical Sciences, Vol. 93, 3004–3012 (2004)

namely site I (also called warfarin binding site) and site II (benzodiazepine binding site). Sjöholm et al.[6] have suggested the existence of one more binding site (digitoxin site). The location of the latter site is largely unknown, but crystallographic studies have assigned the location of sites I and II to subdomains IIA and IIIA of HSA, respectively.[7–9] These assignments are supported by binding studies with fragments of HSA.[10–13]

Detailed studies, mainly competitive binding experiments, have revealed that the binding sites might not be simply constructed but could consist of regions overlapping, or placed close to, each other.[14–17] For example, Fehske et al.[14] have proposed that site I is composed of two overlapping binding regions, namely, the warfarin and azapropazone binding regions. Kragh-Hansen[18] termed this site "a large and flexible region" from the diversity of acceptable ligands and the apparent ability to accommodate more than one of them at a time with significant interference. Recently, we obtained results that strongly support such models: site I consists of at least three regions (Ia, Ib, and Ic) with overlap between Ia and Ib and between Ia and Ic.[19] That is, region Ia locates adjacent to the other regions, as if region Ia has a bridging role between regions Ib and Ic. By contrast, regions Ib and Ic are well separated, because simultaneous ligand binding to these regions apparently takes place in an independent manner. The relation between the three regions and other ligand binding sites as well as the interaction with site II have previously been studied in some detail.[19–22]

The present work was undertaken to further characterize site I focusing on the relationship between regions Ib and Ic. Dansyl-L-asparagine (DNSA) and four chemically related *n*-alkyl *p*-aminobenzoates (*p*-ABEs) (Fig. 1) bind to only one site on HSA, and they were used as probes for region Ib and Ic, respectively.[19] Equilibrium dialysis proposed independent binding to the two regions at all pH values studied (6.0–9.0). By contrast, the highly sensitive spectroscopic techniques circular dichroism (CD) and fluorescence anisotropy could detect interaction between HSA-bound DNSA and *n*-alkyl *p*-ABEs. According to our knowledge, the present findings represent a new type of drug interaction.

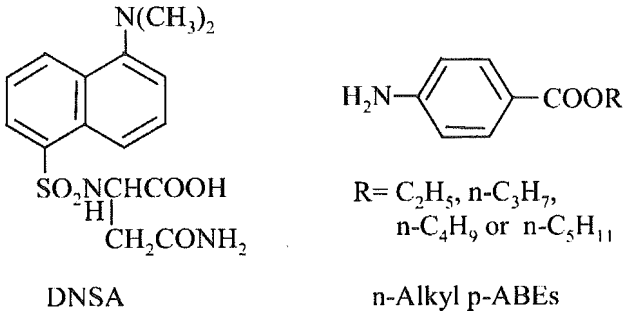

Figure 1. Chemical structures of DNSA and *n*-alkyl *p*-ABEs.

MATERIALS AND METHODS

Materials

HSA was donated by the Chemo-Sera-Therapeutic Research Institute (Kumamoto, Japan). It was defatted with activated charcoal in aqueous solution adjusted to pH 3 with H_2SO_4 at 0°C, dialysed with deionized water and then freeze-dried, as originally described by Chen.[23] The molecular mass of HSA was assumed to be 66,500 Da. HSA gave only one band in sodium dodecyl sulfate-polyacrylamide gel electrophoresis. DNSA was purchased from Sigma Chemical Co. (St. Louis, MO). *n*-Alkyl *p*-ABEs were synthesized by alkylation of *p*-aminobenzoic acid according to a conventional method,[24] and their structures were confirmed by elemental analysis, melting point determination, and nuclear magnetic resonance. All other chemicals were of analytical grade. All buffers used were prepared with sodium phosphate dibasic and sodium phosphate monobasic salts. All ligand molecules were first dissolved in methanol; the final concentration of methanol was less than 1% (v/v).

CD Measurements

CD measurements were made on a Jasco model J-720A spectropolarimeter (Tokyo, Japan), using a 10 mm cell at 25°C. Induced ellipticity was defined as the ellipticity of DNSA-HSA mixture minus the ellipticity of HSA alone within the same wavelength region and was expressed in degrees. No induced ellipticities of *n*-alkyl *p*-ABEs-HSA mixtures were observed at wavelengths longer than 320 nm. Molar ellipticities $[\theta]$ (deg · cm^2 · dmol^{-1}) were calculated from the following formula:

$$[\theta] = \frac{(100 \cdot \theta_{obs})}{l \cdot C} \quad (1)$$

where θ_{obs} is the observed ellipticities, and l and C are path length (centimeters) and molar

concentration of the HSA-DNSA complex (bound DNSA), respectively.

Fluorescence Polarization Technique

Polarized fluorescence was measured on a Jasco FP-770 fluorometer with polarizer attachment (FP-2010) and a thermostatic cuvette holder. Excitation and emission wavelengths for DNSA were 350 and 480 nm, respectively. Polarized fluorescence was obtained as fluorescence anisotropy (r), as shown by the following expression[25]:

$$r = \frac{(I_{\parallel})_V - (I_{\perp})_V \cdot G}{(I_{\parallel})_V + 2(I_{\perp})_V \cdot G} \quad (2)$$

The subscript V refers to vertically polarized excitation beam. $I_{\parallel}$ and $I_{\perp}$ are emission components parallel and perpendicular to the polarized excitation beam, respectively. G is the wavelength-dependent grating correction factor represented by the following equation[26]:

$$G = \frac{(I_{\parallel})_H}{(I_{\perp})_H} \quad (3)$$

The subscript H refers to horizontally polarized excitation beam.

Viscosity of the Medium

Glycerol was used as a viscous medium. The viscosity of the medium was changed by altering the temperature from 20 to 80°C; it was measured by the cone-and-plate microviscometer Contarves Low-Shear 30 (Zurich, Switzerland) thermally controlled.

Equilibrium Dialysis

Equilibrium dialysis experiments were performed using 2-mL Sanko plastic dialysis cells (Fukuoka, Japan). The two cell compartments were separated by Visking cellulose membranes. Aliquots (1.5 mL) of samples were dialyzed at 25°C for 12 h against the same volume of buffer solution. After equilibrium was reached, the concentration of free DNSA in the buffer compartment was determined by high-performance liquid chromatography as follows. The high-performance liquid chromatography system consisted of a Hitachi 655A-11 pump and a Hitachi F1000 variable fluorescence monitor. A LiChrosorb RP-18 (Cica Merck, Tokyo, Japan) column was used as the stationary phase. For DNSA assay, the fluorescence monitor was used. Excitation and emission wavelengths were 330 and 550 nm, respectively. The mobile phase consisted of 5 mM phosphate buffer (pH 7.7)-acetonitrile (77:23 v/v). DNSA adsorption onto membrane or apparatus was negligible because no adsorption was detected on measurement of the DNSA concentrations of both compartments in equilibrium dialysis experiments in HSA-free equilibrium. Binding parameters were estimated by fitting the experimental data to the following equation using a nonlinear least-squares computer program (MULTI program)[27]:

$$\nu = \frac{[D_b]}{[P_t]} = \sum_{i=1}^{j} \frac{n_i K_i [D_f]}{1 + K_i [D_f]} \quad (4)$$

where ν is the number of moles of DNSA bound per mole protein. $[P_t]$ is the protein concentration, and $[D_b]$ and $[D_f]$ are the bound and unbound DNSA concentrations, respectively. K_i and n_i are the association constant and the number of binding sites for the ith class of binding sites.

RESULTS

Characteristics of CD Spectra

Binding of DNSA to HSA at pH 7.4 resulted in an induced negative Cotton effect with a maximal effect around 360 nm (Fig. 2A). Addition of n-alkyl

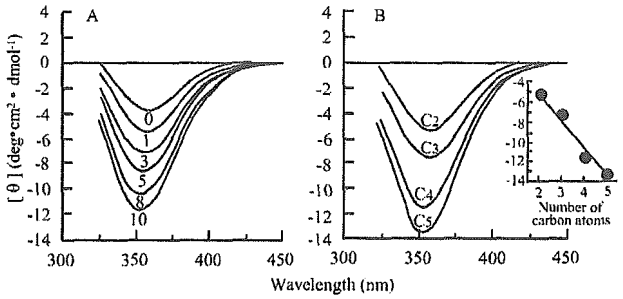

Figure 2. Effects of the concentration of n-butyl p-ABE (A) and alkyl chain length of the n-alkyl p-ABEs (B) on the CD spectrum of the DNSA-HSA system at pH 7.4. The following concentrations were used for HSA and DNSA: HSA, 40 μM; DNSA, 40 μM. The numbers in (A) indicate the concentrations of n-butyl p-ABE as the n-butyl p-ABE to HSA ratio. C2–C5 in (B) represent the numbers of carbon atoms in the alkyl side chain of the n-alkyl p-ABEs. The inset to (B) shows the maximal effect of the number of carbon atoms in the n-alkyl p-ABEs at an n-alkyl p-ABEs to HSA molar ratio of 10.

p-ABEs produced particular effects in the induced CD spectrum of the DNSA-HSA complex. For example, increasing concentrations of *n*-butyl *p*-ABE increased the intensity of the negative CD ellipticity and shifted the maximum wavelength to 350 nm (Fig. 2A). All of the four *n*-alkyl *p*-ABEs had principally the same effect, but the extent of the effects depended on the length of the alkyl side chain (Fig. 2B) and that in a linear manner as illustrated for the ellipticities (see inset to Fig. 2B). Thus, increasing the length of the alkyl side chain resulted in more pronounced CD changes.

Increasing pH from 7.4 to 9.0 caused changes in the CD spectrum of the DNSA-HSA complex which were similar to those induced by addition of the *n*-alkyl *p*-ABEs (Fig. 3). By contrast, decreasing pH from 7.4 to 6.0 resulted in completely different spectral changes: the negative CD ellipticity around 360 nm disappeared, and a new, but smaller, positive CD ellipticity appeared around 320 nm.

The effect of *n*-butyl *p*-ABE binding on the molar ellipticity of DNSA-HSA was investigated at several pHs (Fig. 4). It is seen that, as pH increased, the effect of *n*-butyl *p*-ABE became smaller. Similar findings were obtained for the other *n*-alkyl *p*-ABEs (data not shown). Thus, in all cases, pH caused sigmoidal changes in the ellipticity. Furthermore, maximal effects were registered for pH $\geq$ 7.4 and high concentrations of the *n*-alkyl *p*-ABEs except at pH 9, where no additional effect of the compounds was observed.

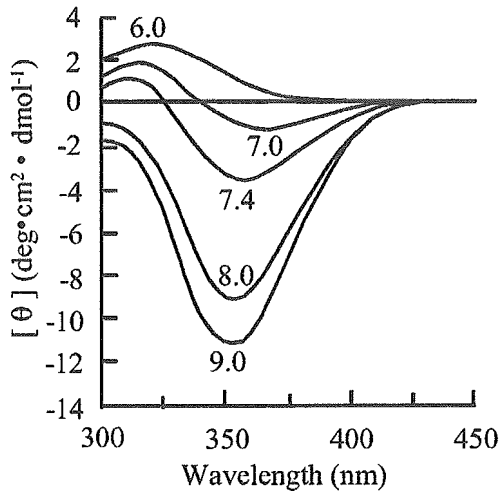

Figure 3. CD spectra of the DNSA-HSA system at various pHs. The numbers 6.0–9.0 represent the pH. The following concentrations were used for HSA and DNSA: HSA, 40 μM; DNSA, 40 μM.

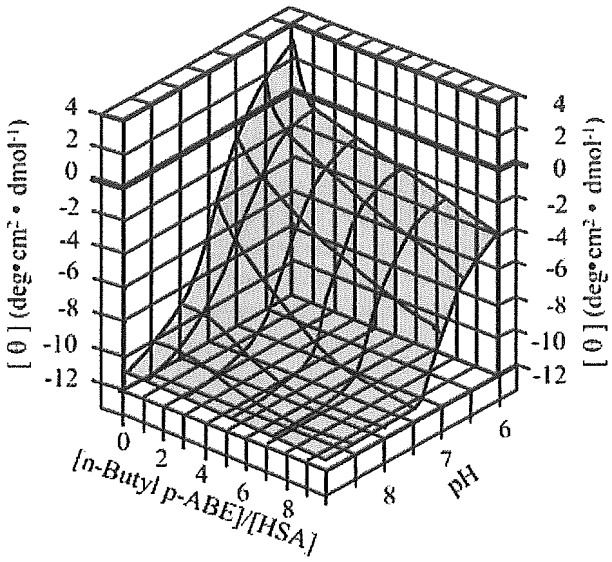

Figure 4. Molar ellipticity of the DNSA-HSA complex in the presence of different *n*-butyl *p*-ABE concentrations and at different pHs. The following concentrations were used for HSA and DNSA: HSA, 40 μM; DNSA, 40 μM. Molar ellipticity was measured at maximum intensity.

Equilibrium Dialysis

The number of binding sites and the corresponding association constants for binding of DNSA to HSA were estimated by using equilibrium dialysis (Tables 1 and 2). It is seen that in all cases binding of DNSA takes place at one high-affinity site. The existence of one high-affinity site is in accordance with previous studies.[19] Addition of different concentrations of *n*-butyl *p*-ABE did not affect binding. Even addition of high concentrations of *n*-butyl *p*-ABE and of the other *n*-alkyl *p*-ABEs (*n*-alkyl *p*-ABEs to HSA molar ratio of 10) did not affect the binding affinity of DNSA (Table 1). By contrast, increasing pH from 6.0 to 9.0 increased the association constant for DNSA by a factor of three without affecting the number of binding sites (Table 2). Thus, pH and the *n*-alkyl *p*-ABEs have different effects on DNSA-HSA binding.

Fluorescence Anisotropy

Fluorescence anisotropy derived from the DNSA-HSA complex was determined to obtain information about the mobility of bound DNSA. As a first step, Figure 5 shows the fluorescence anisotropy of DNSA, in the absence of HSA, as a function of the viscosity of the medium. The double reciprocal plot of fluorescence anisotropy against medium

Table 1. Effects of *n*-Alkyl *p*-ABEs on the Number of Binding Sites (n) and Association Constant (K) for Primary DNSA Binding to HSA at pH 7.4

Type of *n*-alkyl *p*-ABE	[*n*-Alkyl *p*-ABEs]/[HSA]	n	K ($\times 10^5$ M^{-1})
None	0	1.07 ± 0.10	1.81 ± 0.37
Ethyl *p*-ABE	10	0.98 ± 0.15	1.94 ± 0.41
n-Propyl *p*-ABE	10	1.00 ± 0.15	1.92 ± 0.39
	2	1.11 ± 0.13	1.89 ± 0.42
	4	1.01 ± 0.11	1.84 ± 0.33
n-Buthyl *p*-ABE	6	0.98 ± 0.07	1.92 ± 0.25
	8	1.07 ± 0.17	1.82 ± 0.34
	10	1.03 ± 0.15	1.83 ± 0.15
n-Amyl *p*-ABE	10	1.13 ± 0.13	1.87 ± 0.37

The following concentrations were used to estimate the association constant of DNSA: HSA, 40 μM; DNSA, 4–40 μM. Data represent the mean ± SD of three experiments.

viscosity gave a straight line with a good correlation coefficient of 0.999. According to this finding, restriction of fluorescent probe mobility is accompanied by increased fluorescence anisotropy. Addition of increasing concentrations of *n*-butyl *p*-ABE to DNSA-HSA enhanced the fluorescence anisotropy of bound DNSA (Fig. 6). Actually, addition of high concentrations of all the *n*-alkyl *p*-ABEs increased the fluorescence anisotropy, and the mobility restriction of bound DNSA increased linearly with the number of carbon atoms in the alkyl side chain (Fig. 6A, inset). Increments of pH also resulted in enhanced fluorescence anisotropy of bound DNSA, but it did so in a less uniform way: changing pH from 6 to 8 increased fluorescence anisotropy, whereas an additional change to 9 resulted in a small reduction of fluorescence anisotropy (Fig. 6B). The latter finding indicates similar fluorescent probe mobilities at pH 8 and 9.

In summary, the fluorescence anisotropy data were more in agreement with the CD data than with the association constant data. This is especially evident when studying the effect of adding *n*-alkyl *p*-ABEs. These similarities between the CD and fluorescence anisotropic findings might be related to DNSA mobility at the binding region Ib.

Table 2. Effect of pH on the Number of Binding Sites (n) and Association Constant (K) for Primary DNSA Binding to HSA

pH	n	K ($\times 10^5$ M^{-1})
6.0	0.98 ± 0.12	1.37 ± 0.36
7.0	1.11 ± 0.20	1.66 ± 0.25
7.4	1.07 ± 0.15	1.81 ± 0.27
8.0	0.98 ± 0.13	2.95 ± 0.42
9.0	1.03 ± 0.09	4.11 ± 0.40

The following concentrations were used to estimate the association constant of DNSA: HSA, 40 μM; DNSA, 4–40 μM. Data represent the mean ± SD of three experiments.

DISCUSSION

HSA and α_1-acid glycoprotein (AGP) are two important transport and depot proteins in the circulation. AGP is considered to possess only one ligand binding site, consisting of several overlapping regions for exogenous and endogenous substances.[28] HSA has at least three binding sites for high-affinity binding of drugs, namely, site I, site II and site III also called the warfarin,

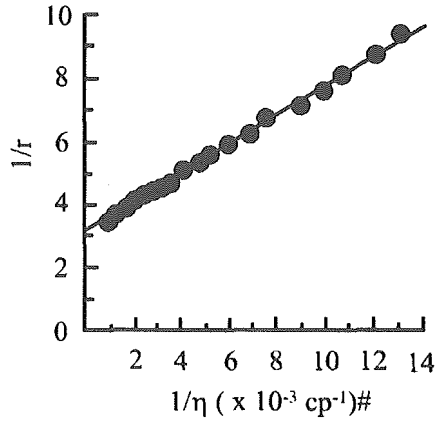

Figure 5. Relation between medium viscosity (η) and DNSA fluorescence anisotropy (r). The relationship is shown in a double reciprocal plot. The correlation coefficient is 0.999. The viscosity of glycerol as a medium is adjusted by temperature changes. #Viscosity is given as centipoise (cp).

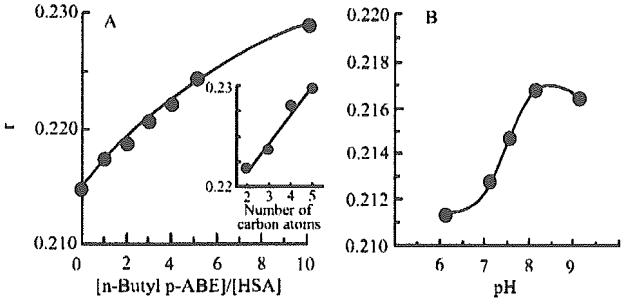

Figure 6. Effects of *n*-butyl *p*-ABE (A) and pH (B) on the fluorescence anisotropy (r) of DNSA bound to HSA. The following concentrations were used for HSA and DNSA: HSA, 40 μM; DNSA, 10 μM. The concentration of *n*-butyl *p*-ABE is represented as the molar ratio to HSA in (A). The inset to (A) indicates the effect of the number of carbon atoms in the *n*-alkyl *p*-ABEs at an *n*-alkyl *p*-ABEs to HSA molar ratio of 10. The experiments of (A) were performed at pH 7.4.

benzodiazepine and digitoxin binding site, respectively.[4–6] At the molecular level, the binding sites of HSA may also consist of several binding regions.[14–17,19] In other words, a binding site might be composed of a group of several regions which are adjacent to or overlapping each other. For example, site I is thought to consist of two (warfarin and azapropazone binding regions)[14] or three regions (regions Ia, Ib, and Ic).[19] In addition, because of differences in bilirubin-displacing effects[15] and in stereoselective binding modes,[16,17] drug binding indicates that also site II can be subdivided into binding regions.

Mutual displacement of drugs is often the result of competitive binding to a site or region at a drug carrier protein. Although drugs that bind to different sites or regions cannot interact directly according to a competitive binding model, indirect effects such as cooperative or anticooperative interaction may change drug binding. For example, the interaction between AGP-bound dicoumarol derivatives and protriptyline has been suggested to be the result of such binding modes.[29] This type of finding leads us to the idea that even though the binding constants for two ligands, as determined by, for example, equilibrium dialysis, are not affected by simultaneous binding, the binding could still be influenced by conformational changes in the protein. For testing this hypothesis, we have studied cobinding of DNSA and *n*-alkyl *p*-ABEs to site I of HSA by both equilibrium dialysis and spectroscopic techniques.

Interaction of HSA and DNSA, which is a probe for region Ib, generated a Cotton effect at around 360 nm at pH 7.4 (Fig. 2). Because unbound DNSA is not optically active, and HSA does not produce any Cotton effects at these wavelengths, the observed Cotton effects must be extrinsic in origin. The extrinsic Cotton effects are thought to result from interaction of ligand chromophore with an asymmetrical locus in the protein.[30–33] Thus, extrinsic Cotton effects reflect the characteristics of specific asymmetrical sites in the protein molecule and could provide information on the microenvironment of binding sites or ligand orientation in the sites. Therefore, Cotton effects produced by the DNSA-HSA interaction are useful for investigating possible relations between region Ib and, for example, region Ic.

Equilibrium dialysis proposed independent binding of DNSA and the *n*-alkyl *p*-ABEs, which are probes for region Ic, at all pH values studied (Table 1 and data not shown). This finding is in accordance with previous analyses of equilibrium dialysis data performed with an equation that included different interaction modes (competitive, independent, cooperative, or anticooperative binding).[19] However, the results of the CD measurements revealed that binding of the *n*-alkyl *p*-ABEs changed the spatial relationship for bound DNSA (Fig. 2). Furthermore, the spectral changes were very similar to those accompanying increments in pH in the region, in which HSA is known to undergo the neutral-to-base transition (N-B transition). In accordance with these findings, the effect of *n*-alkyl *p*-ABEs binding on the CD spectra of the DNSA-HSA system was predominant at pH 6, whereas there was only a very small effect at pH 9 (Fig. 4). The magnitude of the effects of *n*-alkyl *p*-ABEs was dependent on the concentration of the ligand and on the length of the alkyl side chain. It is reasonable to consider that the DNSA molecule takes up the most preferable orientation in the B conformer, because maximal extrinsic Cotton effects were observed at pH 9, and addition of *n*-alkyl *p*-ABEs did not cause further effects on the spatial orientation of DNSA to the asymmetric center in the B conformer. Such a binding model is also in accordance with the finding that DNSA binds with a higher association constant at pH 9 (Table 2). The proposal that the N-to-B transition and *n*-alkyl *p*-ABEs binding cause reorientation of HSA-bound DNSA was supported by fluorescence polarization data, because fluorescence anisotropy derived from the DNSA-HSA complex gives information about the mobility of bound DNSA.[34] The results showed (Fig. 6) that the mobility of DNSA bound to HSA is restricted by

the N-B transition and *n*-alkyl *p*-ABE binding in a similar manner.

Within the pH range used, the association constant for DNSA binding to HSA describes a sigmoidal curve (Table 2, not illustrated). This finding is consistent with other studies using site I ligands.[20,35–37] Therefore, HSA is considered also to take up the N and B conformations at pH 6 and 9, respectively, when complexed with DNSA.

Despite the similarity of the effects of N-B transition and *n*-alkyl *p*-ABE binding on DNSA's spatial orientation, their effects on equilibrium binding, and thereby the binding constant for DNSA, were different. The N-B transition increased DNSA binding, whereas cobinding of the *n*-alkyl *p*-ABEs did not significantly affect DNSA binding. Based on studies with HSA fragments, domains I and II undergo dramatic changes in tertiary structure as the N-B transition proceeds.[38] The proton bindings and releases are considered to be involved in the process of the N-B transition.[35,39] The structural changes involving delayed deprotonation of five histidine residues in domain I and breaking of salt bridges between domains I and III cause increased flexibility of the HSA molecule and tighter binding of ligands to site I in subdomain IIA.[10,11,35,37,40,41] In addition to the N-B transition, HSA undergoes several other transitions in dependence of pH, namely, the N-F transition between pH 5.0 and 3.5 and the F-E transition or acid expansion below pH 3.[8,42] Among these structural transitions, the N-B transition has been proposed to have physiological importance, because it takes place within the pH range of blood plasma,[8,22,35,42,43] and could change not only individual binding of drugs but also ligand-ligand interactions on HSA through changes in spatial relationships between regions or sites.[22,44,45] It is somewhat surprising that, even though the N-B transition affects DNSA binding, it has no influence on the type of interaction between HSA-bound DNSA and *n*-alkyl *p*-ABE, namely, independent binding to site I. Thus, the changes of DNSA's spatial orientation in region Ib caused by the N-B transition and by *n*-alkyl *p*-ABE binding cannot be identical.

A possible scheme for the changes in DNSA's binding and spatial orientation is given in Figure 7. In short, at pH 6, DNSA binds with a relatively low affinity to region Ib; the binding results in a CD spectrum with positive θ values (upper left corner). Increasing pH to 9 modifies the conformation of the binding site which results in high-affinity binding and in a CD spectrum with maximal negative θ values (upper right corner). However, simultaneous binding of an *n*-alkyl *p*-ABE to region Ic at pH 6 does not affect the association constant for DNSA to a detectable degree but affects the orientation of bound DNSA. The latter effect results in a CD spectrum with moderate negative θ values (lower left corner). Finally, independent high-affinity binding of the two types of ligands also takes place at pH 9. Actually, the binding affinity and orientation of bound DNSA, as well as the CD spectrum, are the same, whether *n*-alkyl *p*-ABEs are present or not (lower right corner). For illustration clarity, we have not shown the fluorescence results which, however, are in accordance with the scheme. A final evaluation of the model probably has to be done by X-ray analyses of HSA-ligand crystals.

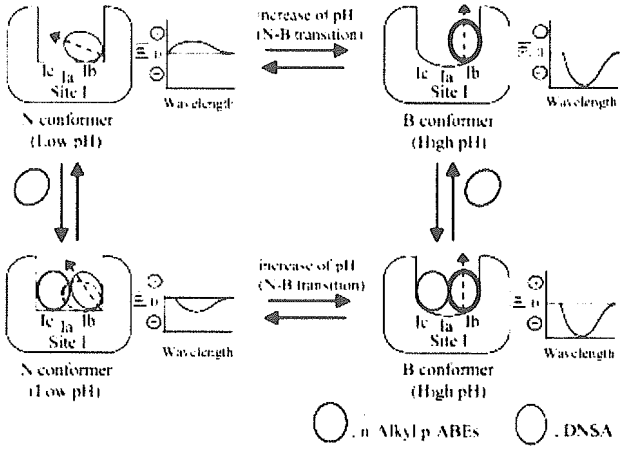

Figure 7. Schematic model of the change in spatial orientation of DNSA in region Ib and of its CD spectrum caused by binding of *n*-alkyl *p*-ABEs to region Ic at different pHs. The dashed arrows indicate the direction of contribution to positive or negative ellipticities on that orientation, and the bold line in the DNSA molecule indicates binding with high affinity.

In conclusion, the results showed that even though one method, for example, equilibrium dialysis, proposes independent binding of two ligands, other methods, for example, CD and fluorescence measurements, can detect interactions between the bound ligands. The results also showed that such interactions can be modulated by structural changes in the protein molecule, for example, those accompanying the N-B transition of HSA. The present findings afford a deep insight into drug binding to site I and a way of looking at a new type of interaction.

REFERENCES

1. Sellers EM, Koch-Weser J. 1977. Clinical implications of drug-albumin interaction. In: Rosenoer VM, Oratz M, Rothschild MA, editors. Albumin structure, function and uses. Oxford, UK: Pergamon Press, pp 159–182.
2. Vallner JJ. 1977. Binding of drugs by albumin and plasma protein. J Pharm Sci 66:447–465.
3. McMenamy RP. 1977. Albumin binding sites. In: Rosenoer VM, Oratz M, Rothschild MA, editors. Albumin structure, function and uses. Oxford, UK: Pergamon Press, pp 143–158.
4. Sudlow G, Birkett DJ, Wade DN. 1975. The characterization of two specific drug binding sites on human serum albumin. Mol Pharmacol 11:824–832.
5. Sudlow G, Birkett DJ, Wade DN. 1976. Further characterization of specific drug binding sites on human serum albumin. Mol Pharmacol 12:1052–1061.
6. Sjöholm I, Ekman B, Kober A, Ljungstedt-Pahlman I, Seiving B, Sjödin T. 1979. Binding of drugs to human serum albumin. XI. The specificity of three binding sites as studied with albumin immobilized in microparticles. Mol Pharmacol 16:767–777.
7. He XM, Carter DC. 1992. Atomic structure and chemistry of human serum albumin. Nature 358: 209–215.
8. Carter DC, Ho JX. 1994. Structure of serum albumin. Adv Protein Chem 45:153–201.
9. Petitpas I, Bhattacharya AA, Twine S, East M, Curry S. 2001. Crystal structure analysis of warfarin binding to human serum albumin: Anatomy of drug site I. J Biol Chem 276:22804–22809.
10. Bos OJ, Remijn JP, Fischer MJ, Wilting J, Janssen LH. 1988. Location and characterization of the warfarin binding site of human serum albumin. A comparative study of two large fragments. Biochem Pharmacol 37:3905–3909.
11. Bos OJ, Fischer MJ, Wilting J, Janssen LH. 1989. Mechanism by which warfarin binds to human serum albumin. Stopped-flow kinetic experiments with two large fragments of albumin. Biochem Pharmacol 38:1979–1984.
12. Dockal M, Carter DC, Ruker F. 1999. The three recombinant domains of human serum albumin. Structural characterization and ligand binding properties. J Biol Chem 274:29303–29310.
13. Dockal M, Chang M, Carter DC, Ruker F. 2000. Five recombinant fragments of human serum albumin-tools for the characterization of the warfarin binding site. Protein Sci 9:1455–1465.
14. Fehske KJ, Schlafer U, Wollert U, Müller WE. 1982. Characterization of an important drug binding area on human serum albumin including the high-affinity binding sites of warfarin and azapropazone. Mol Pharmacol 21:387–393.
15. Maruyama K, Nishigori H, Iwatsuru M. 1985. Characterization of the benzodiazepine binding site (diazepam site) on human serum albumin. Chem Pharm Bull 33:5002–5012.
16. Noctor TAG, Pham CD, Kaliszan R, Wainer IW. 1992. Stereochemical aspects of benzodiazepine binding to human serum albumin. I. Enantioselective high performance liquid affinity chromatographic examination of chiral and achiral binding interactions between 1,4-benzodiazepines and human serum albumin. Mol Pharmacol 42:506–511.
17. Kaliszan R, Noctor TAG, Wainer IW. 1992. Stereochemical aspects of benzodiazepine binding to human serum albumin. II. Quantitative relationships between structure and enantioselective retention in high performance liquid affinity chromatography. Mol Pharmacol 42:512–517.
18. Kragh-Hansen U. 1988. Evidence for a large and flexible region of human serum albumin possessing high affinity binding sites for salicylate, warfarin, and other ligands. Mol Pharmacol 34:160–171.
19. Yamasaki K, Maruyama T, Kragh-Hansen U, Otagiri M. 1996. Characterization of site I on human serum albumin: Concept about the structure of a drug binding site. Biochim Biophys Acta 1295:147–157.
20. Yamasaki K, Miyoshi T, Maruyama T, Takadate A, Otagiri M. 1994. Characterization of region Ic in site I on human serum albumin. Microenvironmental analysis using fluorescence spectroscopy. Biol Pharm Bull 17:1656–1662.
21. Sakai T, Yamasaki K, Sako T, Kragh-Hansen U, Suenaga A, Otagiri M. 2001. Interaction mechanism between indoxyl sulfate, a typical uremic toxin bound to site II, and ligands bound to site I of human serum albumin. Pharm Res 18:520–524.
22. Yamasaki K, Maruyama T, Yoshimoto K, Tsutsumi Y, Narazaki R, Fukuhara A, Kragh-Hansen U, Otagiri M. 1999. Interactive binding to the two principal ligand binding sites of human serum albumin: Effect of the neutral-to-base transition. Biochim Biophys Acta 1432:313–323.
23. Chen RF. 1967. Removal of fatty acids from serum albumin by charcoal treatment. J Biol Chem 242: 173–181.
24. Kadaba PK, Carr M, Tribo M, Triplett J, Glasser AC. 1969. Boron trifluoride ethyl ether as an effective catalyst in the synthesis of alkyl *p*-aminobenzoates. J Pharm Sci 58:1422–1423.
25. Dash D, Rao GR. 1990. Characterization of the effects of propranolol on the physical state of platelet membrane. Arch Biochem Biophys 276:343–347.
26. Chen RF, Bowman RL. 1965. Fluorescence polarization: Measurement with ultraviolet-polarizing filters in a spectrophotofluorometer. Science 147: 729–732.

27. Yamaoka K, Tanigawara Y, Nakagawa T, Uno T. 1981. A pharmacokinetic analysis program (multi) for microcomputer. J Pharmacobiodyn 4:879–885.
28. Maruyama T, Otagiri M, Takadate A. 1990. Characterization of drug binding sites on alpha 1-acid glycoprotein. Chem Pharm Bull 38:1688–1691.
29. Miyoshi T, Yamamichi R, Maruyama T, Takadate A, Otagiri M. 1992. Further characterization of reversal of signs of induced cotton effects of dicumarol derivatives-alpha 1-acid glycoprotein systems by protriptyline. Biochem Pharmacol 43:2161–2167.
30. Chignell CF. 1969. Optical studies of drug-protein complexes. II. Interaction of phenylbutazone and its analogues with human serum albumin. Mol Pharmacol 5:244–252.
31. Chignell CF. 1969. Optical studies of drug-protein complexes. 3. Interaction of flufenamic acid and other *N*-arylanthranilates with serum albumin. Mol Pharmacol 5:455–462.
32. Chignell CF. 1970. Optical studies of drug-protein complexes. IV. The interaction of warfarin and dicoumarol with human serum albumin. Mol Pharmacol 6:1–12.
33. Chignell CF, Starkweather DK. 1971. Optical studies of drug-protein complexes. V. The interaction of phenylbutazone, flufenamic acid, and dicoumarol with acetylsalicylic acid-treated human serum albumin. Mol Pharmacol 7:229–237.
34. Shinitzky M, Barenholz Y. 1978. Fluidity parameters of lipid regions determined by fluorescence polarization. Biochim Biophys Acta 515:367–394.
35. Wilting J, van der Gielsen WF, Jansen LHM, Weideman MM, Otagiri M, Perrin JH. 1980. The effect of albumin conformation on the binding of warfarin to human serum albumin. The dependence of the binding of warfarin to human serum albumin on the hydrogen, calcium, and chloride ion concentrations as studied by circular dichroism, fluorescence, and equilibrium dialysis. J Biol Chem 255:3032–3037.
36. Wanwimolruk S, Birkett DJ. 1982. The effects of N-B transition of human serum albumin on the specific drug-binding sites. Biochim Biophys Acta 709:247–255.
37. Kasai-Morita S, Horie T, Awazu S. 1987. Influence of the N-B transition of human serum albumin on the structure of the warfarin-binding site. Biochim Biophys Acta 915:277–283.
38. Dockal M, Carter DC, Ruker F. 2000. Conformational transitions of the three recombinant domains of human serum albumin depending on pH. J Biol Chem 275:3042–3050.
39. Bos OJ, Labro JF, Fischer MJ, Wilting J, Janssen LH. 1989. The molecular mechanism of the neutral-to-base transition of human serum albumin. Acid/base titration and proton nuclear magnetic resonance studies on a large peptic and a large tryptic fragment of albumin. J Biol Chem 264:953–959.
40. Wilting J, Weideman MN, Roomer ACJ, Perrin JH. 1979. Conformational changes in human serum albumin around the neutral pH from circular dichroic measurements. Biochim Biophys Acta 579:469–473.
41. t'Hart BJ, Wilting J, de Gier JJ. 1986. Evidence for distinct consecutive steps in the neutral to base transition of human serum albumin. Biochem Pharmacol 35:1005–1009.
42. Peters T Jr. 1996. All about albumin: Biochemistry, genetics, and medical applications. San Diego: Academic Press.
43. Leonard WJ, Vijai KK, Foster JF. 1963. A structural transformation in bovine and human plasma albumins in alkaline solution as revealed by rotatory dispersion studies. J Biol Chem 238:1984–1988.
44. Dröge JH, Janssen LH, Wilting J. 1985. A study on the allosteric interaction between the major binding sites of human serum albumin using microcalorimetry. Biochim Biophys Acta 827:396–402.
45. Hagag NG, Bimbaum DW, Darnall DW. 1982. Distances between Tyr-411 and Trp-214 of human serum albumin measured by fluorescence energy transfer: Effects of pH and fatty acids. Fed Proc 41: 1189.

Tryptophan Residues Play an Important Role in the Extraordinarily High Affinity Binding Interaction of UCN-01 to Human α-1-Acid Glycoprotein

Masaaki Katsuki,[1] Victor Tuan Giam Chuang,[1,2] Koji Nishi,[1] Ayaka Suenaga,[1] and Masaki Otagiri[1,3]

Received December 4, 2003; accepted May 5, 2004

Purpose. To investigate the factors that contribute to the exceptionally high affinity binding of UCN-01 to human α_1-acid glycoprotein (hAGP).

Methods. Interactions between UCN-01, UCN-02, and staurosporine with native and chemically modified hAGPs were examined using ultracentrifugation and spectroscopic analysis.

Results. The binding affinity of staurosporine, as well as UCN-02, to hAGP was lower than that of UCN-01 by 20- and 100-fold respectively. The percentage of UCN-01 that binds to hAGP was low at acidic pH but increased with increasing pH, reaching a maximum at pH 7.4. The binding of UCN-01 to desialylated hAGP was comparable to that of hAGP. No significant difference was found for the binding of UCN-01 to F1*S and A variants of hAGP. Chemical modification of the His, Lys, Trp, and Tyr residues caused a decrease in percentage of bound UCN-01. Trp-modified hAGP showed the largest decrease in binding. Tryptophanyl fluorescence quenching results indicate that Trp residues play a prominent role in the binding of UCN-01 to hAGP.

Conclusions. A substituent at position C-7 of UCN-01 appeared to influence the binding specificity of the drug, and Trp residues in hAGP play a prominent role in the high affinity binding of UCN-01 to hAGP.

KEY WORDS: α_1-acid glycoprotein; binding site; drug disposition; UCN-01; variants.

INTRODUCTION

UCN-01 (7-hydroxystaurosporine, Fig. 1), a new anticancer drug with good inhibitory activity against protein kinase C (PKC) and cyclin dependent kinases (CDKs), is a hydroxylated derivative of staurosporine. It has been shown to inhibit the growth of various cultured human and solid tumor cells *in vitro* and *in vivo* (1–3). As a single agent, UCN-01 exhibits two key biochemical effects, namely the accumulation of cells in the G1 phase of the cell cycle and the induction of apoptosis. Both of these effects may be important for its anticancer activity. As a modulator, UCN-01 enhances the cytotoxicity of other anti-cancer drugs such as DNA-damaging agents and anti-metabolite drugs through the putative abrogation of G2 and/or S phase accumulation induced by these anti-cancer agents such as mitomycin C, cisplatin and 5-fluorouracil *in vitro* and *in vivo* (4).

Surprisingly, the pharmacokinetics of UCN-01 after administration in the form of a 72- or 3-h infusion to cancer patients displayed entirely distinctive features that would not have been predicted from the preclinical data. The pharmacokinetics of UCN-01 in experimental animals was characterized by rapid clearance with a large distribution volume. The volume of distribution at steady-state conditions (Vd_{ss}), the systemic clearance (CL_{tot}) and the half-life of elimination ($t_{1/2}$) in dogs, rats, and mice were all within the range of 6–17 L/kg, 0.6–4 L h^{-1} kg^{-1}, and 3–12 h, respectively. In contrast to the large distribution volume and rapid systemic clearance in experimental animals, the distribution volumes (0.0796–0.158 L/kg) and systemic clearance (0.0407–0.252 ml h^{-1} kg^{-1}) in the human patients were found to be extremely low. In addition, the elimination half-lives (253–1660 h) were unusually long (5).

This dramatic species difference with respect to the pharmacokinetics of UCN-01 in humans can, at least in part, be explained by specific high-affinity binding to hAGP (5). Steroid hormones and basic drugs are known to bind tightly to hAGP, with binding constants in the order of 10^6 M^{-1} (6). In comparison to the binding constant for canine AGP which is 1.3×10^7 M^{-1}, the binding constant for UCN-01 to hAGP, 8×10^8 M^{-1}, is the highest value ever reported to date. In contrast, no specific binding could be observed for rat AGP and human serum albumin (5). The results of a physiologic model, mimicking a clinical situation and using rats, suggest that the slow dissociation of UCN-01 from hAGP limits its disposition and elimination (7).

Being a member of the acute-phase protein family, the plasma concentrations of hAGP increase up to 5-fold in various acute-phase responses such as inflammation, cancer, stress, post-surgery, pregnancy and other clinical conditions (8). In addition, hAGP exists as a mixture of two or three genetic variants, namely the A and F1*S variants in the plasma of individuals (9). In the general population, three phenotypes are most frequently observed, namely, F1S/A, F1/A and S/A, depending on the presence of two or three of these variants in plasma. Figure 2 shows the amino acid sequence of the hAGP variants (10–12). The A variant and the F1*S variant differ in their amino acid sequence by at least 22 residues (8). Large differences in the binding of various drugs have been reported for the F1*S *vis-à-vis* the A variant (13), indicating a specific drug transport role for each variant.

Increases in circulating hAGP have been reported to alter the pharmacokinetic disposition and pharmacological action of numerous drugs that bind to it. For example, elevated hAGP is associated with a higher bioavailability, and lower systemic clearance and volume of distribution of HIV protease inhibitors such as saquinavir in AIDS patients (14). On the other hand, increased hAGP levels associated with advanced tumors altered the pharmacokinetics of Imatinib (STI571), a tyrosine kinase inhibitor, in leukemia patients (15). In addition to the fact that hAGP plasma concentrations are increased in certain types of cancers, changes in the expression of genetic variants of hAGP could also occur according to the specific type of cancer (16). Hence, hAGP appears to be an important modulator of drug pharmacokinetics and pharmacodynamics.

[1] Department of Biopharmaceutics, Graduate School of Pharmaceutical Sciences, Kumamoto University, Kumamoto 862-0973, Japan.
[2] Department of Pharmacy, Faculty of Allied Health Sciences, Universiti Kebangsaan Malaysia, Jalan Raja Muda Abdul Aziz, 50300 Kuala Lumpur, Malaysia.
[3] To whom correspondence should be addressed. (e-mail: otagirim@gpo.kumamoto-u.ac.jp)

0724-8741/04/0900-1648/0

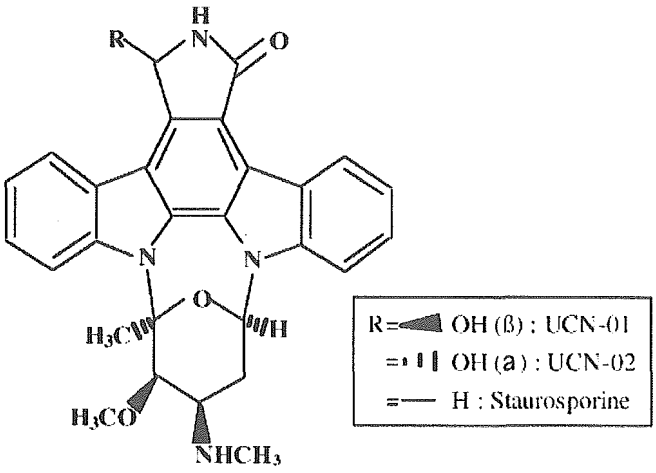

Fig. 1. Chemical structures of UCN-01, UCN-02 and staurosporine.

Since at present no crystallographic structural data for hAGP is available, it becomes important to examine the extraordinarily high affinity binding mechanism between UCN-01 and hAGP using established methods. In this study, we report on the binding interactions between UCN-01 and related compounds with native and chemically modified hAGP using ultracentrifugation and spectroscopic analysis to detect these interactions.

MATERIALS AND METHODS

Materials

UCN-01, UCN-02 and Staurosporine were supplied by Kyowa Hakko Kogyo Co. (Shizuoka, Japan). hAGP (purified from cohn fraction VI) was purchased from Sigma Chemical Co. (St. Louis, MO, USA). Phenylisocyanate and 2-hydroxy-5-nitrobenzyl bromide (HNBB) were purchased from Nacalai Tesque (Kyoto, Japan). Tetranitromethane (TNM) was purchased from Aldrich Chemical Co., Milwaukee, USA. Diethylpyrocarbonate (DEP) and neuraminidase was purchased from Sigma Chemical Co. All other chemicals and solvents were of analytical grade.

Determination of Binding Constant

The binding of UCN-01 to hAGP was determined by an ultracentrifugation technique (17). A constant concentration of hAGP (4 μM) was incubated with different concentrations of UCN-01 (3.2–8 μM). Five ml of an hAGP solution containing UCN-01 was placed in siliconized tubes, along with SIGMACOATE (Sigma), incubation for 10 min on ice, and

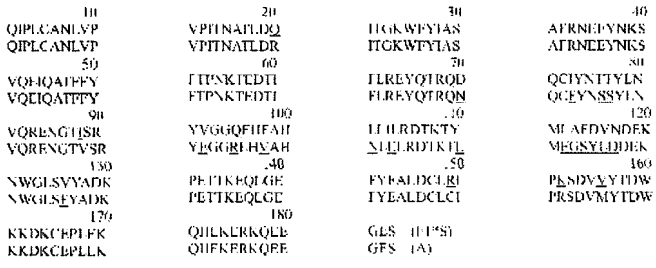

Fig. 2. Amino acid sequence of hAGP variants. Differences in the amino acid sequence between the F1*S and A variant are underlined.

then ultracentrifuged at 225,000 × g for 24 h at 4°C. After ultracentrifugation, an aliquot (50 μl) from the top of the supernatant was used to determine the free UCN-01 concentration by HPLC, as reported previously (18). The unbound fractions were obtained from the supernatant.

Binding parameters were determined by fitting the experimental data to the following Scatchard equation using a non-linear squares program (MULTI program) (19).

$$\frac{r}{D_f} = nK - rK \quad (1)$$

where n is the number of binding sites, K the binding constant, and D_f the free drug concentration, with r denoting the moles of bound ligand per mole of total protein.

Determination of Binding for UCN-01 to hAGP

Percent binding was calculated from the following equation:

$$\text{bound}\ (\%) = \frac{[D_t] - [D_f]}{[D_t]} \times 100 \quad (2)$$

where D_t is the total concentration of UCN-01, the hAGP concentrations were set at 20 μM, and D_f is the free concentration of UCN-01.

Preparation of hAGP Derivatives

Trp-Modified hAGP

The three Trp residues of hAGP were modified by HNBB following the procedure of Fehske *et al.* (20). 40 mg of hAGP was dissolved in 10 ml deionized water adjusted to pH 4.5 with acetic acid. One milliliter of an ethanol solution of HNBB was added to 10 ml of this solution. HNBB was added (100-fold molar excess of hAGP) and the reaction mixture was shaken occasionally. After 2 h the insoluble hydrolyzed reagent was separated by centrifugation. The supernatant was dialyzed against deionized water for 60 h and then lyophilized. The degree of modification was determined using ultraviolet absorption, as shown below.

$$\text{modified}\ (\%) = \frac{A_{410} \times 44100 \times 0.4980}{13800\,(A_{280} - 0.167 \times A_{410})} \times 100 \quad (3)$$

where A_{410} is the maximal absorbance of Trp-modified hAGP, and A_{280} is the maximal absorbance of unmodified hAGP. Of the 3 Trp residues of hAGP, about 1 was modified.

Tyr-Modified hAGP

Modification of the Tyr residues was performed at 4°C according to the procedure of Sokolovsky *et al.* (21). hAGP was dissolved in 10 ml of 0.05 M Tris buffer with a pH of 8.0. A 500-fold molar excess of TNM dissolved in ethanol was added to the hAGP solution. The degree of modification was calculated from the following equation:

$$\text{modified}\ (\%) = \frac{A_{428}}{4100 \times c \times m} \times 100 \quad (4)$$

where A_{428} is the maximal absorbance of Tyr-modified hAGP, c the protein concentration, and m the number of Tyr

residues on an hAGP molecule. Of the 11 Tyr residues of hAGP, about 2 were modified.

Lys-Modified hAGP

Chemical modification of Lys residues was carried out using phenylisocyanate (22). 40 mg of hAGP was dissolved in 10 mL 0.067 M phosphate buffer at pH 7.4. One milliliter of an ethanol solution of phenylisocyanate was added gradually at a 300-fold molar excess over hAGP and the reaction mixture was incubated for 2 h at 4°C, dialyzed against deionized water for 40 h, and then lyophilized. The unreacted Lys residues were determined by the trinitrobenzene sulfonic acid procedure of Haynes *et al.* (23). Of the 14 Lys residues of hAGP, about 4 were modified.

His-Modified hAGP

The His residues were modified with DEP according to the procedure of Roosemont *et al.* (24). 30 mg of hAGP was dissolved in 10 ml of acetate buffer (pH 6.5, 100 mM), DEP in ethanol was then added to the hAGP solution. The ratio of DEP to hAGP was 10. The mixture was stirred for 20 min at 4°C and dialyzed against deionized water and lyophilized. The number of His residues modified was calculated using the following equation:

$$\text{modified}\ (\%) = \frac{A_{240} \times \dfrac{3\ \text{ml}}{\text{ml of test solution}}}{\Delta\varepsilon \times c \times m} \times 100 \qquad (5)$$

where $\Delta\varepsilon$ is the differential molar absorptivity for His at pH 6.0, c the protein concentration and m the number of His residues on hAGP. A_{240} is the maximal absorbance of His-modified hAGP. Of the 3 His residues in hAGP, about 2 were modified.

Separation of hAGP Genetic Variants

The hAGP genetic variants were separated using the method of Herve *et al.* (25). An iminodiacetate (IDA) Sepharose gel loaded with copper (II) ions and equilibrated in buffer 1 (20 mM sodium phosphate buffer, pH 7.0, containing 0.5 M sodium chloride) was packed into a glass column (2.0 × 30.0 cm L, Pharmacia LKB). Commercial hAGP (70 mg dissolved in 1.0 ml of buffer) was applied to the column at a flow rate of 1.0 ml/min. Fractions (10 ml) were collected, and their respective absorbance values were determined spectrometrically at 280 nm. As soon as variant A had been eluted, elution buffer 2 (buffer 1 plus 20 mM imidazole) was applied to the column to remove the bound F1 and S variants (F1/S mixture). The peak fractions of each eluent were collected, concentrated on a YM 10 membrane filter (Amicon, Danvers, MA), dialyzed against deionized water, and lyophilized. The purities of the isolated hAGP preparations were determined by isoelectric focusing (IEF) followed by incubation at 37°C for 24 h with 1 U of neuraminidase (25).

Desialylation of hAGP

hAGP was desialylated enzymatically, using the methodology described by Primozic and McNamara (26), using an immobilized neuraminidase obtained from *Clostridium perfringens*. hAGP (40 mg) was dissolved in 5 ml of 0.067 M phosphate buffer (pH 7.4) and 2 U of enzyme were added. The mixed solution was incubated at 37°C, with gentle stirring at 60 rpm for 24 h after incubation, the mixture was centrifuged and filtered to remove the immobilized enzyme. A small part of the filtrate was used to measure sialic acid by the thiobarbituric acid method. The product was dialyzed against deionized water and the dialysate was lyophilized. Approximately 95% of the sialic acid was removed, leaving an average of one sialic acid residue per protein molecule. The molecular weight of desialylated hAGP was therefore 40000.

Circular Dichroism (CD) Spectra

Circular dichroism spectra were recorded with a JASCO J-720 spectropolarimeter, using 10 μM hAGP in 20 mM buffer at 25°C. Near-UV spectra were recorded using a 10-mm path length cell, and a 0.1-mm path length cell was used for far–UV spectra. Prior to recording the spectra, samples were mixed by vortexing and then incubated for 30 min at room temperature. The mean residue ellipticity [θ], was calculated using the following equation:

$$[\theta] = \frac{\theta}{10 \times c \times 1} \qquad (6)$$

where θ (deg) is the observed ellipticity, l the cell length (cm).

$$c = nCp \qquad (7)$$

where n is the number of amino acid residues and Cp the concentration (mol/L).

Tryptophanyl Fluorescence Spectrum

Fluorescence was measured using a Jasco FP-770 fluorometer (Tokyo, Japan). The excitation wavelength of hAGP was 295 nm, and fluorescent wavelength, 340 nm. The relative fluorescence intensity was calculated using the fluorescence quenching method.

Statistical Analysis

All data are presented as means ± SD. Statistical analysis of difference was determined by one-way ANOVA followed by the modified Fisher's least sequares difference method.

RESULTS

Binding Parameter of UCN-01 Analogs to hAGP

UCN-01 is a novel derivative of staurosporine that is hydroxylated C-7, and UCN-02 is a stereoisomer at C-7 of UCN-01. UCN-01, UCN-02 and staurosporine have been shown to inhibit PKC with IC50 (μM) values of 0.0041, 0.062 and 0.0027, respectively, and to inhibit protein kinase A (PKA) with IC50 (μM) values of 0.042, 0.25, and 0.0082, respectively (27).

Table I shows the binding affinity constants, K_a, of UCN-01 analogues for hAGP. The K_a of UCN-01 for hAGP, 288 ± 75 × 10^6 M^{-1}, is the highest among the three compounds, and is in agreement with previously reported values (5). The K_a for staurosporine where hydrogen is the substituent at C-7 position is about one-twentieth. UCN-02 with an α-hydroxyl group at the C-7 position shows the smallest binding constant among the three ligands, compared to UCN-01. It is interest-

Table I. Binding Parameters of UCN-01, UCN-02, and Staurosporine to hAGP at pH 7.4

	Ligand		
	UCN-01	UCN-02	Staurosporine
K_a ($\times 10^6$ M^{-1})	288 ± 75	1.48 ± 0.11	11.33 ± 5.74
n	0.92 ± 0.04	0.93 ± 0.06	0.91 ± 0.11

All values are mean ± SD (n = 3).

ing to note that a change in the configuration of the hydroxyl group or a substitution of a hydrogen atom at the C-7 position of UCN-01 caused a 20- to 100-fold decrease in binding affinity.

Effect of pH on Binding of UCN-01 to hAGP

The binding of ligands to hAGP is known to be a pH sensitive process (28). The percentage of binding of UCN-01 to hAGP at different pHs, namely 6, 7, 7.4, and 8, was investigated (Fig. 3). The maximum binding of UCN-01 to hAGP occurs at pH 7.4 (96.33%). The binding of UCN-01 to hAGP was found to decrease in both acidic and basic pH values, where the lowest percentage binding was observed at pH 6 (69.74%).

Near-UV CD Spectra of hAGP in Various pHs

Structural profiles of hAGP at pH 6, 7, 7.4, and 8 were investigated by circular dichroism measurements. CD spectra measured at the near UV region reflects conformation or tertiary structure of a protein, while that measured at the far UV region reflects secondary structure. A change in the shape of a CD spectra measured under different conditions in comparison to a reference spectra of a particular set of conditions usually indicates a change in the conformation of the protein. The secondary structures of hAGP were essentially unchanged within the range of pH 6–8 (data not shown), but the tertiary structure changed significantly, as shown in the near UV CD spectra in Fig. 4. These results suggested that the conformational change in the tertiary structure of hAGP is pH dependent. Such a conformational change could affect the microenvironment of binding sites, thus causing a change in the binding of UCN-01 to hAGP.

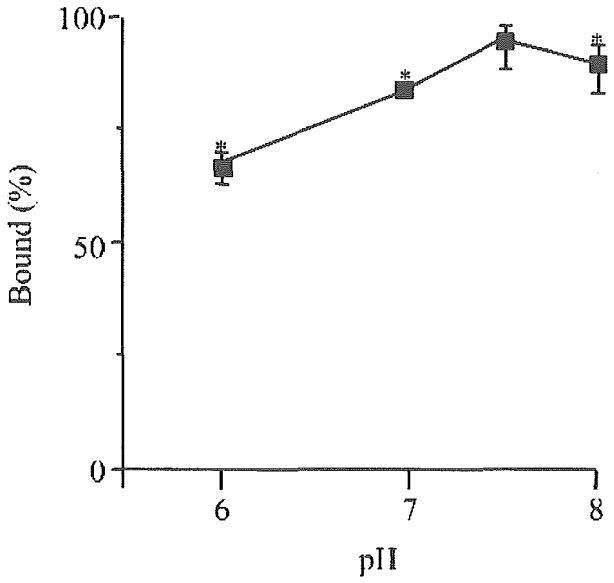

Fig. 3. Effect of pH on the binding of UCN-01 to hAGP. Concentrations are: [UCN-01] = [hAGP] = 20 μM. Each point represents the mean ± SD (n = 3). *Statistically significant compared with pH 7.4; $p < 0.01$.

Effect of Sialic Acid on the Binding of UCN-01 to hAGP at pH 7.4

The carbohydrate terminal chains of hAGP glycans are highly sialylated, containing up to 14 sialic acid residues (29). Therefore, hAGP has a low pKa (=2.6) and isoelectric point (=2.7). Sialic acid residues have been reported to influence the binding of several drugs to hAGP (30). In order to elucidate the role of sialic acid in the binding of UCN-01, we prepared desialylated hAGP and examined the binding percentage of UCN-01 to native and desialylated hAGP, which were 96.33 ± 1.26 and 95.59 ± 1.06, respectively. This suggested that the binding of UCN-01 to desialylated hAGP is comparable to that of native hAGP.

Binding Affinity of UCN-01 to hAGP Variants at pH 7.4

We separated the F1*S and A variants from the hAGP mixture and examined the percentage binding of UCN-01 to each of the variants. As shown in Table II, (the binding percentage of UCN-01 to native, F1*S and A variants are 96.33 ± 1.26, 95.08 ± 0.3 and 95.23 ± 0.45, respectively) there is no significant difference in the binding percent of UCN-01 to the F1*S and A variants of hAGP.

Near-UV CD Spectra of Chemical Modified hAGP and the Effects of the Chemical Modification on Binding of UCN-01 to hAGP

UCN-01 has a very high affinity to hAGP. This high affinity is thought to be derived from not only the hydrophobic interaction but also largely from the electrostatic interac-

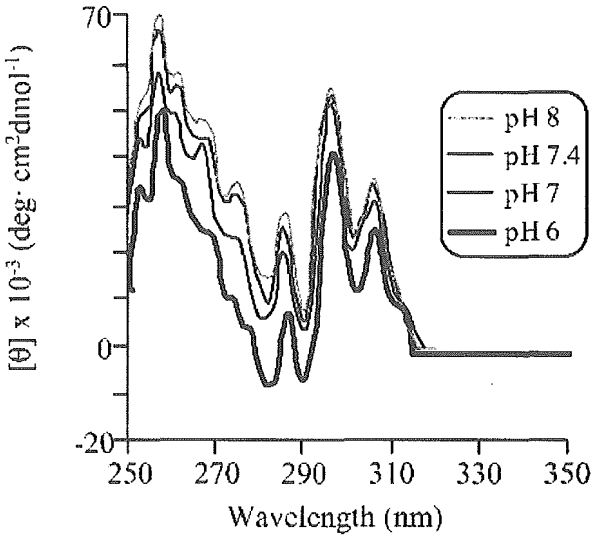

Fig. 4. Near-UV CD spectra of hAGP at various pHs The concentration is: [hAGP] = 10 μM.

Table II. Binding Percentage of UCN-01 to hAGP Variants at pH 7.4

	hAGP		
	Native	F1*S	A
Binding percentage (%)	96.33 ± 1.26	95.08 ± 0.3	95.23 ± 0.45

The concentrations are: [hAGP] = [F1*S] = [A] = [UCN-01] = 20 μM.
All values are means ± SD (n = 3).

tion between UCN-01 and hAGP. In actual fact, binding of UCN-01 to hAGP was affected by the presence of sodium chloride and fatty acid (data not shown). In order to evaluate the role of amino acid residues involved in the binding, we compared the binding of UCN-01 with chemically modified hAGPs. Chemical modification of His, Lys, Trp and Tyr residues of hAGP caused a marked decrease in the binding of UCN-01, with the modification of Trp residues showing the greatest extent of decrease (Table III). In addition, we also measured the binding percentage of staurosporine to these four chemically modified hAGPs and similar results were obtained where modification of Trp residues caused a marked decrease in the binding of staurosporine (data not shown). The CD spectra of His, Lys, Trp, and Tyr residues modified hAGP indicated that the secondary structure of all modified hAGPs hardly change (data not shown), but the tertiary structure changed significantly, particularly in the case of Trp residue modified hAGP (Fig. 5). The fluorescence quenching titration curve of UCN-01 binding to hAGP as shown in Fig. 6 indicated that tryptophan residues may play an important role in the binding of UCN-01 to hAGP.

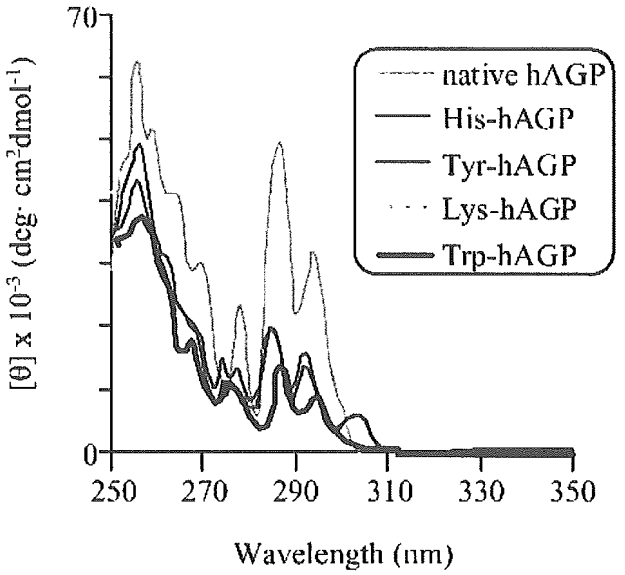

Fig. 5. Near-UV CD spectra of modified hAGPs at pH 7.4 The concentration is: [modified hAGPs] = 10 μM.

DISCUSSION

The initial treatment protocol for UCN-01 was a 72-h infusion administered at 2-week intervals. However, the clinical outcome of the first nine patients treated using this schedule demonstrated unexpectedly high concentrations of drug with a long terminal elimination half-life ($t_{1/2}$). This led to a modification of the UCN-01 administration schedule, in which the recommended phase II dose of UCN-01 is administered as a 72-h continuous infusion at 42.5 mg m^{-2} day^{-1} over a 3 day period. Subsequent courses are administered at 4-week intervals during a 36-h period (31). The extremely low clearance and small distribution volume of UCN-01 in humans could be partly due to the high degree of binding to hAGP. Although many drugs that associate with hAGP have K_a values of 10^5 to 10^6 M^{-1}, UCN-01 is unique in the tightness of its binding to hAGP, with K_a of 10^8 M^{-1}. As a consequence of this extraordinary high binding affinity, a low volume of distribution, which approximates the extracellular volume, and long $t_{1/2}$ is observed. In view of its altered pharmacokinetics due to its high interaction affinity with hAGP, the plasma levels of the hAGP are a potentially important factor in clinical treatment considerations.

hAGP is a glycoprotein that consists of 183 amino acid residues and five carbohydrate chains. The five highly sialylated complex-type-N-linked glycans contribute 45% of the molecular weight (32,33). As an acute phase reactant, hAGP's "basal" level is approximately 20 μmol/L, but it can vary from a 5- to a 10-fold range in response to stress, infection, or the effects of neoplasm in evocation of an inflammatory response. In addition, the levels of hAGP vary widely heterogeneous in cancer patients where the composition of hAGP is heterogeneous according to the type of disease, consisting of different isoforms and degrees of glycosylation. Differences in the binding of drugs to the two main genetic variants of hAGP have also been reported (25). Thus, the distribution of UCN-01 on the hAGP isoforms may also be difficult to predict.

Previous studies indicated that hAGP has one common drug binding site, which appears to be wide and flexible (34). In general, studies in our laboratory have shown that electrostatic and hydrophobic interactions are important driving forces for the binding of ligands to hAGP (35). In a study using fluorescence and ultracentrifugation experimental methods, the binding site of UCN-01 on hAGP was concluded to partly overlap with the binding site for basic drugs, acidic drugs, as well as steroid hormones (18). In order to

Table III. Binding Percentage of UCN-01 to Native and Chemically Modified hAGP at pH 7.4

	Chemically modified hAGP				
	Native	His	Lys	Trp	Tyr
Binding percentage (%)	96.33 ± 1.26	70.44 ± 2.68*	75.97 ± 1.56*	56.97 ± 2.06*	73.70 ± 1.01*

The concentrations are: [UCN-01] = [hAGP] = [chemically modified hAGP] = 20 μM.
All values are mean ± SD (n = 3).
* Statistically significant compared with native hAGP; $p < 0.01$.

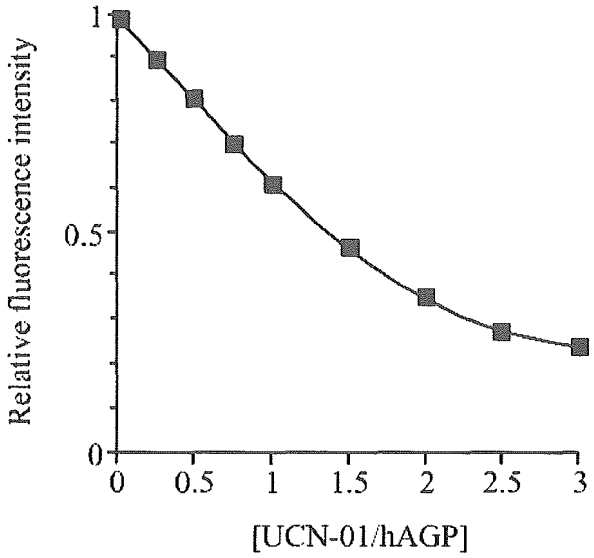

Fig. 6. Fluorescence quenching titration curve of UCN-01 binding to hAGP at pH 7.4 Concentration is: [hAGP] = 1 μM. [UCN-01] = 0 to 3 μM.

examine the ligand-binding site structural relationship of UCN-01 interactions with hAGP, the binding affinity of UCN-01, staurosporine, the "lead" compound among PKC inhibitors and UCN-02, a UCN-01 stereoisomer and weak PKC inhibitor were measured (Fig. 1). The decrease in the binding affinity followed the sequence of UCN-01 > Staurosporine > UCN-02 (Table I). It is obvious that the substituent at the C-7 position of the staurosporine molecule governs the binding affinity of UCN-01 analogues to hAGP. Interestingly, a hundred fold difference in binding affinity was recorded between UCN-01 and UCN-02, suggesting strict stereoisomeric or steric binding requirements of the UCN-01 binding site on hAGP. Meanwhile, the importance of the moiety at the C-7 position has also been reported for binding to target proteins (36,37). In a recent study, the crystal structures of staurosporine and UCN-01 in a complex with the kinase domain of PDK1 showed that, although staurosporine and UCN-01 interact with the PDK1 active site in an overall similar manner, the UCN-01 7-hydroxy group, which is not present in staurosporine, generates direct and water-mediated hydrogen bonds with active-site residues (36). On the other hand, hydrophobic interactions and hydrogen-bonding interactions were observed in the crystal structures between UCN-01 and the Chk1 kinase domain. The selectivity of UCN-01 toward Chk1 over cyclin-dependent kinases is due to the presence of a hydroxyl group in the lactam moiety, that interacts with the ATP-binding pocket. The high structural complementarity of these interactions is consistent with the potency and selectivity of UCN-01 (37). The interaction of the substituent at the C-7 position of UCN-01 to its binding protein is very important in terms of the selectivity of pharmacological activity and binding affinity, as is also the case of its binding to hAGP. It is, thus, apparent that the 7-hydroxy group of UCN-01 may play a key role in abnormally strong binding for hAGP.

The binding interactions of a series of basic ligands with hAGP were reported to increase with increasing pH. It was proposed that hydrophobic interactions dominate the high-affinity binding to hAGP (28). Meanwhile, Taheri *et al.* proposed a binding site for local anesthetics on F1*S of hAGP that is largely comprised of a structurally accommodating hydrophobic pocket, perhaps with the ability to form hydrogen bond to H-donor and -acceptor groups on the ligand and with a basic residue, mostly charged at neutral pH, that is located close to the aromatic group on bound drug molecules (38). In the present binding study, the binding of UCN-01 to hAGP also increased with increasing pH and the maximum binding of UCN-01 to hAGP was observed at pH 7.4 (96.33%). On the other hand, a low percentage of binding percentage was observed at pH 6 (69.74%) (Fig. 3). It is known that a tumor micro-environment is frequently more acidic by approximately 0.3–0.5 pH units, compared with that of its surrounding normal tissues. A decrease in the binding of UCN-01 in an acidic environment may partly contribute to the generation of free UCN-01 molecules for its anticancer activity at the cancer tissues.

hAGP exists in a variety of sialylated states which can be influenced by certain disease states. In a study investigating the effect of the sialylation state of hAGP on the binding of a model cationic drug, propranolol, the use of desialylated hAGP resulted in a modest increase in the propranolol free fraction (26). Since the binding percentage of UCN-01 to hAGP is more than 95%, an increase in the free fraction could be of clinical importance. Therefore, the binding of UCN-01 to native and desialylated hAGP was determined by ultracentrifugation. The percentage binding of desialylated hAGP was found to be comparable to that of native hAGP, suggesting that the influence of sialylation on UCN-01 binding is negligible. While asialoglycoprotein including desialylated hAGP is commonly known to be internalised by hepatocytes via receptor-mediated endocytosis, staurosporine has been reported to be an effective inhibitor of a liver uptake mechanism such as this (39). Since the liver is the major organ for the metabolism of desialylated hAGP, the significance of such protein trafficking inhibition by UCN-01 in contributing to its own low clearance deserves further investigation.

hAGP plasma concentrations differ depending on the type of cancers and such changes in the expression of the genetic variants of hAGP can be observed in various types of cancer. hAGP can be produced as three main genetic variants, the A variant and the F1 and S variants, which are encoded by two different genes (Fig. 2). Differences in the binding of ligands to hAGP variants have been reported. The ligand binding site of the F1*S variant is reported to be a relatively large hydrophobic pocket that is able to accommodate a variety of chemical structures, whereas the A variant binding site appears to be of smaller size and has a greater ligand specificity. The selective binding of disopyramide and methadone to the A variant and the preferential binding of dipyridamole to the F1*S variant mixture have been reported. On the other hand, lignocaine and chlorpromazine showed a slight preference for binding to the A variant and to the F1*S mixture, respectively. However, progesterone showed no selectivity with regard to any of the variants of hAGP (13). In the present study, no significant difference was detected for the binding of UCN-01 to the F1*S and A variants of hAGP (Table II). Hence, a change in the composition of the variants of hAGP may not be of clinical significance, despite the significant species difference in UCN-01 binding, in which a subsequent administration of hAGP to rats that had been infused

with UCN-01 actually caused a redistribution of the drug back to the blood stream from the peripheral tissues (40).

Chemical modification of His, Lys, Trp and Tyr residues of hAGP caused a marked decrease in the binding of UCN-01 (Table III). The binding percentage of UCN-01 to Trp-modified hAGP was also the lowest among all of the modified samples (Table III). Furthermore, modification of Trp residues also caused a marked decrease in the binding of staurosporine (data not shown). It is obvious that Trp residues are important in maintaining the tertiary structure of hAGP which is necessary for the high affinity binding of UCN-01. In addition, results of binding to chemically modified hAGP suggested that at least one Trp residue is involved in the binding of UCN-01 to hAGP. The involvement of Trp residues in UCN-01 binding could also be observed in the tryptophanyl fluorescence spectra where increasing UCN-01 concentrations led to a decrease in the fluorescence intensity of Trp residues of hAGP (Fig. 6). Interestingly, all three Trp residues are conserved in both F1*S and A variants of hAGP (Fig. 2) which showed no binding discrimination for UCN-01 (Table II).

Although we managed to identify the key factors for the unusually high binding affinity between UCN-01 and hAGP, namely the substituent at C-7 of the UCN-01 molecule and the Trp residues of hAGP, evidence is still lacking for suggesting a direct interaction between these two major factors. Among the three Trp residues of hAGP, two are relatively shielded from the bulk solvent, while the third Trp residue is located on the periphery of the domain (41). Trp^{25} has been deduced to be located deep in the binding pocket while Trp^{122} in the central hydrophobic pocket of the protein (42). Therefore, Trp^{160} could be the one that is exposed to the bulk solvent. Quantification of the chemical modification in the present study showed that, on average, about one Trp residue per mole of hAGP was modified. Since the modification of Trp residues was carried out under mild conditions without a surfactant present, the possibility of Trp^{160} being the modified residue is high. This suggests that Trp^{160} is the Trp residue that is involved in the binding of UCN-01. The identification of the specific Trp residue of hAGP involved in the high affinity binding of UCN-01 is currently underway in our laboratory. UCN-01 represents an initial candidate for a differentially selective protein kinase inhibitor. The results of this study will help in the informed design of future second generation approaches, as well as to serve as basis for further exploration of the potential of staurosporine pharmacophores which could lead to opportunities for structure-based optimization of PDK1 inhibitors.

ACKNOWLEDGMENTS

We wish to thank Kyowa Hakko Kogyo Co. (Shizuoka, Japan) for providing us UCN-01, UCN-02 and staurosporine to carry out the experiments in this study.

REFERENCES

1. S. Akinaga, K. Gomi, M. Morimoto, T. Tamaoki, and M. Okabe. Antitumor activity of UCN-01, a selective inhibitor of protein kinase C, in murine and human tumor models. *Cancer Res.* **51**: 4888–4892 (1991).
2. S. Akinaga, K. Nomura, K. Gomi, and M. Okabe. Effect of UCN-01, a selective inhibitor of protein kinase C, on the cell-cycle distribution of human epidermoid carcinoma, A431 cells. *Cancer Chemother. Pharmacol.* **33**:273–280 (1994).
3. C. M. Seynaeve, M. Stetler-Stevenson, S. Sebers, G. Kaur, E. A. Sausville, and P. J. Worland. Cell cycle arrest and growth inhibition by the protein kinase antagonist UCN-01 in human breast carcinoma cells. *Cancer Res.* **53**:2081–2086 (1993).
4. A. M. Senderowicz. Small-molecule cyclin-dependent kinase modulators. *Oncogene* **22**:6609–6620 (2003).
5. E. Fuse, H. Tanii, N. Kurata, H. Kobayashi, Y. Shimada, T. Tamura, Y. Sasaki, Y. Tanigawara, R. D. Lush, D. Headlee, W. D. Figg, S. G. Arbuck, A. M. Senderowicz, E. A. Sausville, S. Akinaga, T. Kuwabara, and S. Kobayashi. Unpredicted clinical pharmacology of UCN-01 caused by specific binding to human alpha1-acid glycoprotein. *Cancer Res.* **58**:3248–3253 (1998).
6. Z. H. Israili and P. G. Dayton. Human alpha-1-glycoprotein and its interactions with drugs. *Drug Metab. Rev.* **33**:161–235 (2001).
7. E. Fuse, A. Hashimoto, N. Sato, H. Tanii, T. Kuwabara, S. Kobayashi, and Y. Sugiyama. Physiological modeling of altered pharmacokinetics of a novel anticancer drug, UCN-01 (7-hydroxystaurosporine), caused by slow dissociation of UCN-01 from human alpha1-acid glycoprotein. *Pharm. Res.* **17**:553–564 (2000).
8. K. Schmid. In F.W. Putman (ed.), *The Plasma Proteins, Structure, Function and Genetic Control 1*, Academic Press, New York, 1975 pp. 183–288.
9. I. Yuasa, S. Weidinger, K. Umetsu, K. Suenaga, G. Ishimoto, B. C. Eap, J. C. Duche, and P. Baumann. Orosomucoid system: 17 additional orosomucoid variants and proposal for a new nomenclature. *Vox Sang.* **64**:47–55 (1993).
10. L. Dente, G. Ciliberto, and R. Cortese. Structure of the human alpha 1-acid glycoprotein gene: sequence homology with other human acute phase protein genes. *Nuc. Acids Res.* **13**:3941–3952 (1985).
11. L. Dente, M. G. Pizza, A. Metspalu, and R. Cortese. Structure and expression of the genes coding for human alpha 1-acid glycoprotein. *EMBO J.* **6**:2289–2296 (1987).
12. C. M. Merritt and P.G. Board. Structure and characterisation of a duplicated human alpha 1 acid glycoprotein gene. *Gene* **66**:97–106 (1988).
13. F. Herve, G. Caron, J. C. Duche, P. Gaillard, N. Abd Rahman, A. Tsantili-Kakoulidou, P. A. Carrupt, P. d'Athis, J. P. Tillement, and B. Testa. Ligand specificity of the genetic variants of human alpha1-acid glycoprotein: generation of a three-dimensional quantitative structure-activity relationship model for drug binding to the A variant. *Mol. Pharmacol.* **54**:129–138 (1998).
14. J. W. Holladay, M. J. Dewey, B. B. Michniak, H. Wiltshire, D. L. Halberg, P. Weigl, Z. Liang, K. Halifax, W. E. Lindup, and D. J. Back. Elevated alpha-1-acid glycoprotein reduces the volume of distribution and systemic clearance of saquinavir. *Drug Metab. Dispos.* **29**:299–303 (2001).
15. C. Gambacorti-Passerini, M. Zucchetti, D. Russo, R. Frapolli, M. Verga, S. Bungaro, L. Tornaghi, F. Rossi, P. Pioltelli, E. Pogliani, D. Alberti, G. Corneo, and M. D'Incalci. Alpha 1 acid glycoprotein binds to imatinib (STI571) and substantially alters its pharmacokinetics in chronic myeloid leukemia patients. *Clin. Cancer Res.* **9**:625–632 (2003).
16. J. C. Duche, S. Urien, N. Simon, E. Malaurie, and I. Monnet. and J. Barre. Expression of the genetic variants of human alpha-1-acid glycoprotein in cancer. *Clin. Biochem.* **33**:197–202 (2000).
17. P. A. Bombardt, J. E. Brewer, and M. G. Johnson. Protein binding of tirilazad (U-74006) in human, Sprague-Dawley rat, beagle dog and cynomolgus monkey serum. *J. Pharmacol. Exp. Ther.* **269**:145–150 (1994).
18. N. Kurata, S. Matsushita, K. Nishi, H. Watanabe, S. Kobayashi, A. Suenaga, and M. Otagiri. Characterization of a binding site of UCN-01, a novel anticancer drug on alpha-acid glycoprotein. *Biol. Pharm. Bull.* **23**:893–895 (2000).
19. K. Yamaoka, Y. Tanigawara, T Nakagawa, and T. Uno. A pharmacokinetic analysis program (multi) for microcomputer. *J. Pharmacobiodyn.* **4**:879–885 (1981).
20. K. J. Fehske, W. E. Muller, and U. Wollert. The modification of the lone tryptophan residue in human serum albumin by 2-hydroxy-5-nitrobenzyl bromide. Characterization of the modified protein and the binding of L-tryptophan and benzodiazepines to

the tryptophan-modified albumin. *Hoppe Seylers Z. Physiol. Chem.* **359**:709–717 (1978).
21. M. Sokolovsky, J. F. Riordan, and B. L. Vallee. Tetranitromethane. A reagent for the nitration of tyrosyl residues in proteins. *Biochemistry* **5**:3582–3589 (1966).
22. H. Fraenkel-Conrat. Methods for Investigating the Essential Groups for Enzyme Activity. *Methods Enzymol.* **4**:247–269 (1957).
23. R. Haynes, D. T. Osuga, and R. E. Feeney. Modification of amino groups in inhibitors of proteolytic enzymes. *Biochemistry* **6**:541–547 (1967).
24. J. L. Roosemont. Reaction of histidine residues in proteins with diethylpyrocarbonate: differential molar absorptivities and reactivities. *Anal. Biochem.* **88**:314–320 (1978).
25. F. Herve, E. Gomas, J. C. Duche, and J. P. Tillement. Evidence for differences in the binding of drugs to the two main genetic variants of human alpha 1-acid glycoprotein. *Br. J. Clin. Pharmacol.* **36**:241–249 (1993).
26. S. Primozic and P. J. McNamara. Effect of the sialylation state of alpha 1-acid glycoprotein on propranolol binding. *J. Pharm. Sci.* **74**:473–475 (1985).
27. I. Takahashi, Y. Saitoh, M. Yoshida, H. Sano, H. Nakano, M. Morimoto, and T. Tamaoki. UCN-01 and UCN-02, new selective inhibitors of protein kinase C. II. Purification, physico-chemical properties, structural determination and biological activities. *J. Antibiot. (Tokyo)* **42**:571–576 (1989).
28. S. Urien, F. Bree, B. Testa, and J. P. Tillement. pH-dependence of warfarin binding to alpha 1-acid glycoprotein (orosomucoid). *Biochem. J.* **289**:767–770 (1993).
29. K. Schmid, R. B. Nimerg, A. Kimura, H. Yamaguchi, and J. P. Binette. The carbohydrate units of human plasma alpha1-acid glycoprotein. *Biochim. Biophys. Acta* **492**:291–302 (1977).
30. M. H. Rahman, T. Miyoshi, K. Sukimoto, A. Takadate, and M. Otagiri. Interaction mode of dicumarol and its derivatives with human serum albumin, alpha 1-acid glycoprotein and asialo alpha 1-acid glycoprotein. *J. Pharmacobiodyn.* **15**:7–16 (1992).
31. E. A. Sausville, S. G. Arbuck, R. Messmann, D. Headlee, K. S. Bauer, R. M. Lush, A. Murgo, W. D. Figg, T. Lahusen, S. Jaken, X. Jing, M. Roberge, E. Fuse, T. Kuwabara, and A. M. Senderowicz. Phase I trial of 72-hour continuous infusion UCN-01 in patients with refractory neoplasms. *J. Clin. Oncol.* **19**:2319–2333 (2001).
32. J. M. Kremer, J. Wilting, and L. H. Janssen. Drug binding to human alpha-1-acid glycoprotein in health and disease. *Pharmacol. Rev.* **40**:1–47 (1988).
33. M. J. Treuheit, C. E. Costello, and H. B. Halsall. Analysis of the five glycosylation sites of human alpha 1-acid glycoprotein. *Biochem. J.* **283**:105–112 (1992).
34. T. Miyoshi, R. Yamamichi, T. Maruyama, A. Takadate, and M. Otagiri. Further characterization of reversal of signs of induced cotton effects of dicumarol derivatives-alpha 1-acid glycoprotein systems by protriptyline. *Biochem. Pharmacol.* **43**:2161–2167 (1992).
35. T. Miyoshi, R. Yamamichi, T. Maruyama, and M. Otagiri. Reversal of signs of induced cotton effects of dicumarol-alpha 1-acid glycoprotein systems by phenothiazine neuroleptics through ternary complexation. *Pharm. Res.* **9**:845–849 (1992).
36. D. Komander, G. S. Kular, J. Bain, M. Elliott, D. R. Alessi, and D. M. Van Aalten. Structural basis for UCN-01 (7-hydroxystaurosporine) specificity and PDK1 (3-phosphoinositide-dependent protein kinase-1) inhibition. *Biochem. J.* **375**:255–262 (2003).
37. B. Zhao, M. J. Bower, P. J. McDevitt, H. Zhao, S. T. Davis, K. O. Johanson, S. M. Green, N. O. Concha, and B. B. Zhou. Structural basis for Chk1 inhibition by UCN-01. *J. Biol. Chem.* **277**:46609–46615 (2002).
38. S. Taheri, L. P. Cogswell, A. Gent, and G. R. Strichartz. Hydrophobic and ionic factors in the binding of local anesthetics to the major variant of human alpha1-acid glycoprotein. *J. Pharmacol. Exp. Ther.* **304**:71–80 (2003).
39. R. J. Fallon and M. Danaher. The effect of staurosporine, a protein kinase inhibitor, on asialoglycoprotein receptor endocytosis. *Exp. Cell Res.* **203**:420–426 (1992).
40. N. Kurata. Pharmacokinetics and pharmacodynamics of a novel anti-cancer drug, indrocarbazole analogue, UCN-01. Ph.D. Thesis, Kumamoto University, Japan (2000).
41. M. L. Friedman, K. T. Schlueter, T. L. Kirley, and H. B. Halsall. Fluorescence quenching of human orosomucoid. Accessibility to drugs and small quenching agents. *Biochem. J.* **232**:863–867 (1985).
42. T. Kute and U. Westphal. Steroid-protein interactions. XXXIV. Chemical modification of alpha1-acid glycoprotein for characterization of the progesterone binding site. *Biochim. Biophys. Acta* **420**:195–213 (1976).

Drug Metab. Pharmacokin. 19 (4): 297–302 (2004).

Regular Article

Kinetic Studies of Covalent Binding between N-acetyl-L-cysteine and Human Serum Albumin Through a Mixed-disulfide Using an N-methylpyridinium Polymer-based Column

Daisuke HARADA[1], Makoto ANRAKU[2], Hikaru FUKUDA[2], Shinsaku NAITO[1], Kumiko HARADA[2], Ayaka SUENAGA[2] and Masaki OTAGIRI[2]

[1]*Division of Pharmacology, Drug Safety and Metabolism, Otsuka Pharmaceutical Factory, Inc., Tokushima, Japan*
[2]*Graduate School of Pharmaceutical Sciences, Kumamoto University, Kumamoto, Japan*

Full text of this paper is available at http://www.jssx.org

Summary: The binding properties of the disulfide covalent bond between N-acetyl-L-cysteine (NAC) and human serum albumin (HSA) were investigated. HSA, purified from either healthy subjects or renal failure patients, was incubated with NAC in buffer and analyzed by 4VP-EG-Me column chromatography, which can distinguish between the redox states of the only free thiol of HSA. Although intact HSA was found to consist of mainly three sub-types, marcaptoalbumin (HMA), cysteine-bound nonmercaptoalbumin (HNA_{Cys}) and a further oxidized form (HNA_{oxy}), the formation of a new type of nonmercaptoalbumin (HNA_{NAC}) was confirmed after incubation with NAC. Interestingly, NAC rapidly dissociated Cys from HNA_{Cys} and NAC itself bound very slowly to HSA. These findings suggest that the interaction between NAC and HSA proceeds in a 2-step processes. The first-order binding and dissociation rate constants of NAC to healthy HSA ($k_{on,NAC}$) and Cys from healthy HNA_{Cys} ($k_{off,Cys}$) were approximately 0.0032 and 1.3 (h^{-1}), respectively. On the other hand, HSA from renal failure patients showed decreased HMA and increased HNA_{Cys}. The $k_{on,NAC}$ and $k_{off,Cys}$ were 0.0094 and 0.45 (h^{-1}), respectively, suggesting that the pathological state may affect the binding properties of HSA and NAC.

Key words: human serum albumin; N-acetyl-L-cysteine; covalent binding; disulfide bond; kinetics

Introduction

Human serum albumin (HSA) contains a free thiol that can interact outside of the albumin molecule and is derived from a cysteine residue at the 34th amino acid (Cys^{34}).[1] HSA can bind various thiol-containing compounds *via* a mixed-disulfide bond, which forms between the free thiol of Cys^{34} and a thiol from the other compound. Studies using various thiol-containing drugs have shown that the formation and degradation of such covalent bonds proceeds not instantaneously but time-dependently and that the covalent-binding ratio between the thiol-containing drug and albumin varies with time.[2-5] Therefore, elucidation of the properties of such protein-drug binding over time is an important pharmacokinetic issue in order to understand the efficacy of thiol-containing drugs.

We previously reported the kinetic profiles of covalent binding between albumin and N-acetyl-L-cysteine (NAC), which is a thiol-containing drug used as a mucolytic agent, by determining the free- and protein-bound drug concentrations.[4,5] On the other hand, Narazaki *et al.* have reported kinetic and mechanical profiles of the binding between HSA and other thiol-containing drugs, such as Captopril and Bucillamine, by directly detecting the conformational changes of the Cys^{34} moiety of albumin using *N*-methylpyridinium polymer-based (4VP-EG-Me) column chromatography.[2,3]

In the present study, we directly quantified HSA using a 4VP-EG-Me column after incubation with NAC and analyzed the kinetic properties of covalent protein binding in order to obtain basic information on the covalent binding between HSA and NAC. In addition, we investigated the effect of pathological conditions on binding kinetics of NAC using HSA purified from the

Received; May 22, 2004, Accepted; June 25, 2004
To whom correspondence should be addressed: Daisuke HARADA, *Division of Pharmacology, Drug Safety and Metabolism, Otsuka Pharmaceutical Factory, Inc., 115 Aza kuguhara, Tateiwa, Muya-cho, Naruto, Tokushima 772-8601, Japan. Tel. +81-88-685-1151, Fax. +81-88-686-8176, E-mail: haradada@otsukakj.co.jp*